

Harnessing Unrecognizable Faces for Face Recognition

Siqi Deng Yuanjun Xiong Meng Wang Wei Xia Stefano Soatto
Amazon AWS AI

{siqideng, yuanjx, mengw, wxia, soattos}@amazon.com

Abstract

The common implementation of face recognition systems as a cascade of a detection stage and a recognition or verification stage can cause problems beyond failures of the detector. When the detector succeeds, it can detect faces that cannot be recognized, no matter how capable the recognition system. Recognizability, a latent variable, should therefore be factored into the design and implementation of face recognition systems. We propose a measure of recognizability of a face image that leverages a key empirical observation: An embedding of face images, implemented by a deep neural network trained using mostly recognizable identities, induces a partition of the hypersphere whereby unrecognizable identities cluster together. This occurs regardless of the phenomenon that causes a face to be unrecognizable, it be optical or motion blur, partial occlusion, spatial quantization, poor illumination. Therefore, we use the distance from such an “unrecognizable identity” as a measure of recognizability, and incorporate it in the design of the overall system. We show that accounting for recognizability reduces the error rate of single-image face recognition by 58% at $FAR=1e-5$ on the IJB-C Covariate Verification benchmark, and reduces the verification error rate by 24% at $FAR=1e-5$ in set-based recognition on the IJB-C benchmark.

1. Introduction

We aim at making face recognition systems easier to use responsibly. This requires not just reducing the error rate, but also producing interpretable performance metrics, with estimates of when recognition can be performed reliably, or otherwise should not be attempted, or deemed unreliable.

In most face recognition systems, each image is first fed to a face detector (FD), that returns the location and shape of a number of bounding boxes likely to portray faces. Those, together with the image, are then fed to a downstream face recognition (FR) module that returns either one of K labels corresponding to identities in a database (search), or a binary label corresponding to whether or not the bounding box matches a given identity (verification). FD and

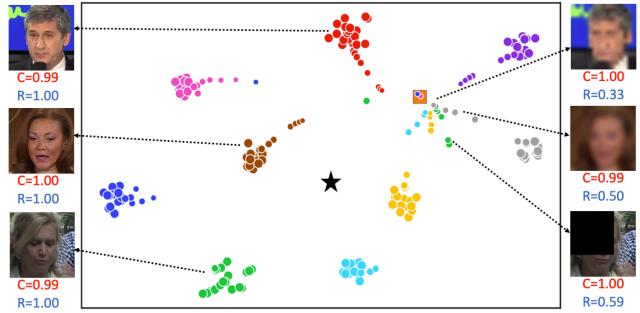


Figure 1. Hypersphere embeddings [34] of different faces from the IJB-C dataset (colored clusters) visualized as circles with area proportional to recognizability, using t-SNE [22]. As the images are perturbed artificially, becoming increasingly unrecognizable, their embeddings migrate to join a common cluster (orange square). Such an “unrecognizable identity” (UI) is described in Sec. 2.2.1 and distinct from the centroid of the recognizable embeddings (black pentagram). Note the difference between *face detection confidence* (C) and *embedding based recognizability score* (R). The former is the output of a face detector and measures the likelihood that the image contains a face while the latter measures if the face can be recognized.

FR are typically non-interacting modules trained on different datasets: The FD is tasked with finding faces no matter whether they are recognizable. The FR is tasked with mapping each detection onto one of K identities. An obvious failure mode of such cascaded systems is when the FD is *wrong*: If a face is not detected, obviously it cannot be correctly recognized. If a detected bounding box does not show a face, the FR system will nonetheless map it to one of the known identities, unless post-processing steps are in place, typically involving a threshold on some confidence measure.

Even when the FD is *right*, there remain the following problems:

First, while an image may contain enough information to decide that there *is* a face, it may not contain enough to determine *whose* face it is, regardless of how good the FR system is. This creates a gap between the FD, tasked to determine that there is a face regardless of whether it is rec-

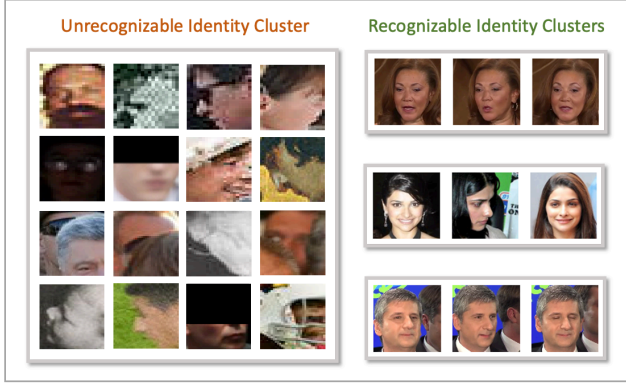


Figure 2. During face clustering, faces with low recognizability scores are grouped into one cluster by distance based clustering method (left), compared with clusters of faces with known identities (right). We refer to this cluster as unrecognizable identity cluster (UI) cluster. The UI cluster including images subject to occlusion, optical or motion blur, low resolution, poor illumination, etc. So the clustering of UIs is not simply due to visual similarity.

ognizable, and the FR, tasked to recognize it. An FR system should not try to recognize a face that is not recognizable.

¹ Accordingly, *how can we measure and account for recognizability of a face image in face recognition?*

Second, failure to take into consideration recognizability can lead to misleading results in face recognition benchmarks. Unrecognizable faces due to optical, atmospheric, or motion blur, spatial quantization, poor illumination, partial occlusion etc, are typically used to train and score FD systems, but FR systems are trained using recognizable faces, lest one could not establish ground truth. Accordingly, *how can we balance the reward in detecting unrecognizable faces with the risk in failure to recognize them?*

Third, failure to account for recognizability of a face can have consequences beyond the outcome of FR on that face. Consider the problem of set-based face recognition where the identity is to be assigned *not* to a single image, but to a small collection of images known to come from the same identity, some of which unrecognizable. These may be frames of a video, some of which affected by motion blur or partial occlusions. It may seem that using all the available data can only improve the quality of the decision. However, uniform averaging can significantly degrade performance. Accordingly, *how should one combine images in set-based face recognition, assuming we have available a measure of recognizability?*

¹An optimal (Bayesian) FR system would forgo the FD and marginalize over all possible locations and shapes, which is obviously intractable. But conditioning on the presence of a face, rather than marginalizing it, is not the only problem: There is another latent variable, “*recognizability*” that is unaccounted for and instead assumed to be true by the FR.

1.1. Main Hypothesis and Empirical Observation

The three questions above point to the need to explicitly represent “*recognizability*” as a latent variable. As was the case for the FD, marginalization is impractical. We instead hypothesize that recognizability can be quantified inferentially. A measure of recognizability could then be used to complete the hypothesis space for FR, effectively adding an additional class for *unrecognizable identities*, akin to open-set classification. An estimate of recognizability would also allow us to correctly weight the influence of the detector in the overall FR results. Finally, recognizability would allow proper weighting of different samples in set-based face recognition.

So, recognizability and the addition of an unrecognizable identity (UI) class would address the issues set forth in the introduction. But *what is the unrecognizable identity?* Is it an actual identity, or just a moniker for the connected interstitial space around the decision boundaries among all known identities?

If we represent each face via an embedding in a compact metric space, such as the hypersphere, perturbing the image until it is unrecognizable moves the corresponding embedding close to a decision boundary. So, it is reasonable to expect that the embeddings of UIs distribute along the boundaries of decision regions with no particular relation to each other: Distant identities, when perturbed, would become distant UIs. Instead, we observe the following phenomenon: *When training a FR system without any UIs, and using the resulting embedding to cluster identities (both recognizable and not), UIs cluster together in representation space*, despite being unrecognizable versions of different identities that may otherwise be far in representation space.

This phenomenon, illustrated in Fig. 1, is counter-intuitive at many levels: First, UIs do not distribute near the boundary between different identities, but rather close to each other and far from the corresponding identities. This happens without imposing any loss on the distance among UIs – for they are not even included in the training set for the FR – and likely made possible by the geometry of the high-dimensional hypersphere.² Second, this phenomenon is not engendered by “low-quality” images of UI being *similar to each other*, enough to form their own cluster. Unlike other domains where motion blurred images form their own cluster, distinct from the low-resolution cluster, here the UI cluster is *highly heterogeneous*, with images that exhibit occlusion, optical or motion blur, low resolution, poor illumination, etc. So, the clustering of UIs is not simply due to visual similarity. Sample of these phenomena are illustrated in Fig. 2 and Sec. 2.2.1. We conjecture that this behavior is specific to FR, which is a fine-grained category

²This phenomenon is unrelated to the known collapse of representations of low-quality images towards the origin of a linear embedding space [24], as here the embedding is constrained to be on the hypersphere.

rization task, where nuisance variability can cause coarse-grained perturbations that move the corresponding samples out-of-domain.

We are now ready to tackle the main goal: Leverage the key empirical observation above to *harness unrecognizable faces to improve face recognition*.

1.2. Contributions and Related Work

Our contribution is three-fold, corresponding to the three questions posed in the introduction:

1) We propose a measure of recognizability that leverages the existence of a single UI cluster in the learned embedding. The “*embedding recognizability score*” (ERS) is simply the Euclidean (chordal) distance of the embedding of an image from the center of UI cluster in the hypersphere.

2) We use the ERS to mitigate the detrimental effect of using different datasets for FD and FR. This results in 58% error reduction (at FAR=1e-5 on the IJB-C Covariate Verification benchmark) in single-image face recognition, without impacting the performance of the detector.

3) We propose an aggregation method for set-based face recognition, by simply calculating the weighted average relative to the ERS, and report 24% error reduction (at FAR=1e-5 on IJB-C) compared with uniform averaging.

We emphasize that unrecognizable faces are still included in the evaluation and the improvement is due to the proposed matching criteria using ERS (Sec. 2.2.2).

The face recognition literature is gargantuan; by necessity, we limit our review to the most closely related methods, cognizant that we may omit otherwise important work. Like most, we use a deep neural network (DNN) model to compute our embedding function mapping an image x and a bounding box b to a (pseudo-)posterior score $\phi(x_b) \propto \log P(y|x, b)$ where $y \in \{1, \dots, K\}$ denotes the identity for the case of search, and $K = 2$ for verification [7, 8, 15, 38, 25, 29, 20, 35, 43, 21, 36, 14]. Our work relates to efforts to understand the effect of image quality on face recognition: Some explicitly modeled image quality in face aggregation [9, 39, 40, 41, 18], others utilized correlation among images from the same person to improve set-based [16, 17] or video-based [27] face recognition. More recently, [11, 12] developed face quality assessment tools and methods [32], probabilistic representation to model data uncertainty [31, 1, 30], as well as explicit handling of quality variations with sub-embeddings [31].

1.3. Implications on Bias and Fairness

As any data-driven algorithmic method, a trained FR system is subject to statistical bias due to the distribution of the training set, and more general algorithmic bias engendered by the choice of models, inference criteria, optimization method, and interface. In addition to those externalities, there can be intrinsic sources of bias that exist before any al-

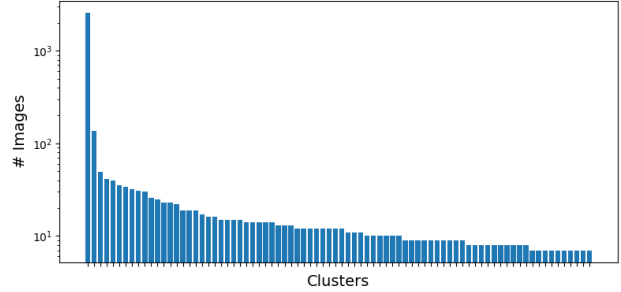


Figure 3. Clustering results on WIDER Face [42] dataset. Cluster sizes are shown in descending order, y-axis in log-scale. The first clusters is larger than the other clusters by two or more orders of magnitude, and are full of miscellaneous low-recognizability images.

gorithm is implemented or dataset collected: Light interacts with matter in a way that depends on sub-surface scattering properties of materials, which is different depending on skin color and affects recognizability by *any* system, natural or artificial. Moreover, clothing, hairdo, makeup, and accessories similarly can impact recognizability. We therefore expect that the UI will *not* represent an unbiased sampling of the population and reflect physical and phenomenological characteristics of the scene, the illuminant, the sensor, and the capture method, regardless of the algorithm used to infer recognizability. *In addition*, recognizability is based on statistical properties of embedding, which is subject to the usual data and algorithmic biases. It is not clear how to balance different populations in the UI. We defer these important and delicate questions to the many studies on bias and fairness, and focus on the independent question of how to deal with recognizability irrespective of what algorithm or system is used for recognition.

2. Face recognizability in face recognition

2.1. Observing Recognizability

The observation that **unrecognizable identities cluster together** can be illustrated using face embeddings [34] on images of 8 randomly sampled celebrities from the IJB-C dataset. We synthesize unrecognizable images by perturbing images with increasing Gaussian blur, motion blur, and occlusions. The t-SNE visualization of the embeddings is shown in Fig. 1, where recognizable faces form separate clusters corresponding to their identities, but as they become increasingly unrecognizable they do not distribute around the boundary between identities, nor around their centroid, but rather around a distinct cluster, the “unrecognizable identity (UI)”.

To validate this result, we perform clustering [4] on faces detected by a state-of-the-art FD model on the WIDER-Face [42] dataset. A heterogeneous cluster emerges, com-

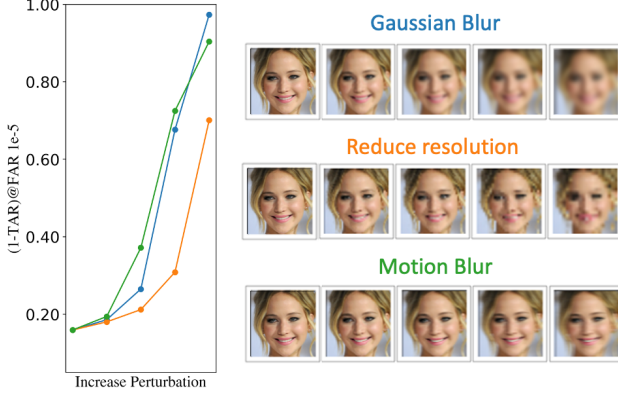


Figure 4. Face verification accuracy can be heavily impacted by image perturbation when we test on IJB-C Template-based Face Verification benchmark: left x-axis marks perturbation level low to high and y-axis marks the error rate $(1-\text{TAR})$ at $\text{FAR}=1e^{-5}$, in correspondence with images on the right side, perturbation types are color-coded.

posed of solely unrecognizable and visually dissimilar faces. The number of images in this cluster is larger than most of the other clusters by more than two orders of magnitude, as can be observed from the histogram in Fig. 3. The phenomenon that identity-agnostic UI images distribute closely in one cluster and away from identity-based clusters could explain two typical types of face quality related errors in FR reported in several prior works [1, 30]: false positive matches between two low-quality faces of different ids, and false negative matches between high and low-quality faces of the same id. The fact that *the UI is distant from other recognizable identities in the embedding space*, also suggests a way of *measuring recognizability by measuring their distances to the UI* as we detail in Sec. 2.2.1.

The face clustering results are surprising as low-quality non-face images (for instance, a quality degraded ImageNet [6] database) ordinarily tend to cluster by appearance: blurred images form a cluster which is distinct from that of dark images, and that of motion-blurred images, etc. We conjecture that the existence of UI has to do with the fine-grained nature of the face domain, because we discover similar phenomena also emerge in other fine-grained recognition tasks like person re-identification (re-id) benchmark Market1501 [44] and a fashion product retrieval dataset Deepfashion [19].

What impact could the UIs have on the downstream FR task? To quantify this, we add three types of image corruption: Gaussian blur, reduced resolution and linear motion blur, to images of the IJB-C face verification benchmark. Then we measure the change of verification error and show the results in Fig. 4. We observe a clear trend of verification error increase as more corruption is added. This shows the risk of not considering the recognizability of the images in



Figure 5. Sample images from IJB-C dataset, grouped by embedding based recognizability score (ERS): high (>0.95), middle ($0.7-0.8$), and low (<0.6). Images with low ERS are hard to recognize even for human viewers.

recognition and calls for a mitigation solution.

2.2. Accounting for Recognizability

Based on the hypothesis that distance to the UI cluster centroid could serve as a measure of the face recognizability, we use the distance as an *embedding recognizability score* (ERS), which requires no additional training nor annotation, and can be easily incorporated into both single-image and set-based face recognition.

2.2.1 The Embedding Recognizability Score (ERS)

We define Embedding Recognizability Score (ERS) to be the distance between an embedding vector and the average embedding of UI images. We utilize the WIDERFace [42] FD dataset to obtain a large amount of UI images. After running clustering algorithm on faces in the dataset, we take the largest resultant cluster which contains only unrecognizable images (Fig. 3). The normalized average embedding of this cluster, \mathbf{f}_{UI} , is then used to represent the UI. Given an embedding vector \mathbf{f}_i , its ERS e_i is defined as

$$e_i = \min(1 - \langle \mathbf{f}_{UI}, \mathbf{f}_i \rangle, 1). \quad (1)$$

We illustrate the correlation between ERS and recognizability in Fig. 5 by taking images from the IJB-C dataset and grouping them by their ERS scores. The ERS decrease is accompanied by face quality variations such as occlusion distortion, larger pose and increased image blurriness.

2.2.2 ERS in Single-Image Based Recognition

Face verification aims to determine whether two face images, x_1 and x_2 , belong to the same person. The face embedding model represents an input face image x_i as the feature vector $\mathbf{f}_i \in \mathcal{R}^d$. Without considering recognizability, the decision function $V : (\mathcal{R}^d, \mathcal{R}^d) \rightarrow [0, 1]$ is

$$V(\mathbf{f}_1, \mathbf{f}_2) = \mathbb{1}(s(\mathbf{f}_1, \mathbf{f}_2) \geq \tau). \quad (2)$$

Here $s(\cdot, \cdot)$ is the cosine similarity function and $\mathbb{1}(\cdot)$ is the indicator function. This decision function predicts the

two images are from the same person ($V(\mathbf{f}_1, \mathbf{f}_2) = 1$) when their similarity score is above the threshold τ . To take ERS into account, we change the decision function to $V' : (\mathcal{R}^d, \mathcal{R}^d, \mathcal{R}, \mathcal{R}) \rightarrow [0, 1]$ as

$$V'(\mathbf{f}_1, \mathbf{f}_2, e_1, e_2) = \mathbb{1}(s(\mathbf{f}_1, \mathbf{f}_2) \geq \tau) \mathbb{1}(e_1 \geq \gamma) \mathbb{1}(e_2 \geq \gamma). \quad (3)$$

Here we introduce an additional threshold γ for the ERS. The rationale is that when the face is unrecognizable (low ERS), it is safer to predict “different identity” than “the same identity”, due to the high empirical risk of false acceptance against false rejection in face verification, especially considering those caused by the UI cluster.

Face identification aims to tell whether one query image x_i , represented as \mathbf{f}_i belongs to one of N indexed identities in the gallery, represented as $\{\mathbf{g}_j\}_{j=1}^N$.³ Here we assume that the gallery has mostly recognizable images. Without considering recognizability, the decision function $S(\mathcal{R}^d) \rightarrow [0, \dots, N]$ is

$$S(\mathbf{f}_i; \{\mathbf{g}_j\}) = \mathbb{1}[\max_j s(\mathbf{f}_i, \mathbf{g}_j) \geq \tau] \cdot \arg \max_{j=1, \dots, N} s(\mathbf{f}_i, \mathbf{g}_j). \quad (4)$$

The query has a positive match when the maximal similarity score to any of the gallery images is above the threshold τ . With ERS, the decision function becomes

$$S'(\mathbf{f}_i; \{\mathbf{g}_j\}) = S(\mathbf{f}_i; \{\mathbf{g}_j\}) \mathbb{1}(e_i \geq \gamma). \quad (5)$$

We predict no positive match when the query image’s recognizability is below the threshold γ . If there is no guarantee that the gallery images are mostly recognizable images, similar to Eq. 3, ERS threshold could be applied to both the gallery and the query.

2.2.3 ERS in Image Set-based Face Recognition

In set-based face recognition, we have prior knowledge that each set or template [23], contains one or multiple face images belonging to a single person. Set-based face recognition also usually consists of two tasks, face verification and face identification. We first extract feature vectors using the embedding model for every image in each set θ_i containing images $\{x_i^l\}$ as $\{\mathbf{f}_i^l\}_{l=1}^{|\theta_i|}$, where $|\theta_i|$ is the cardinality of θ_i . Then the feature vectors are aggregated into one feature vector \mathbf{f}_i . After aggregation, the processing is the same as in the single image case. We design an aggregation function weighted by the ERS of each image as

$$\mathbf{f}_i = \sum_{l=1}^{|\theta_i|} \frac{w(e_i^l) \mathbf{f}_i^l}{\sum_l e_i^l}, \quad e_i = \frac{\sum_l e_i^l}{|\theta_i|}, \quad (6)$$

³In this work we only deal with the “open-set” setting [23] where it is allowed to predict that a query has no match in the gallery, as it is the most common usage in real-world face recognition systems.

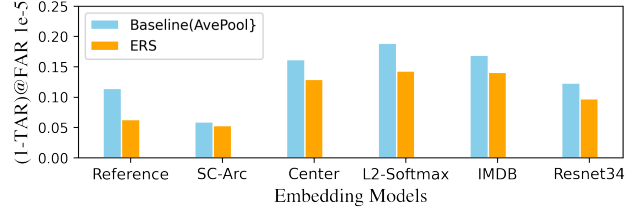


Figure 6. Pairwise performance comparison between baseline (average pooling) and our method (ERS) on IJB-C template across different settings, our method achieves consistent error reduction. Training settings are as follows: Reference (ResNet101 + CosFace Loss + DeepGlintFace), SC-Arc (ResNet101 + Sub-center Arcface Loss + DeepGlintFace), Center (ResNet101 + Softmax+Center Loss + DeepGlintFace), L2-Softmax (ResNet101 + ℓ_2 -Softmax Loss + DeepGlintFace), IMDB (ResNet101 + CosFace Loss + IMDB), ResNet34 (ResNet34 + CosFace Loss + DeepGlintFace).

where \mathbf{f}_i and e_i denote the aggregated feature vector and ERS for the set θ_i , $w : \mathcal{R} \rightarrow \mathcal{R}^+$ denotes the weighting function based on ERS. Combining Eq. 6 into Eq. 3 and Eq. 5 we can obtain the decision rules for the two tasks. We experiment with different choices of weighting function in Sec. 3.

3. Experiments

We examine the effectiveness of ERS in face recognition on multiple benchmarks. We consider two face image quality assessment methods as the baselines: FaceQnet [12] and SER-FIQ [32]. In set-based face recognition, we compare the ERS based aggregation function with other set-based recognition methods: NAN [41], Multicolumn [40], DCN [39], PFE [30] and DUL [1].

Implementation details. We use the deep learning framework MXNet [2] in our model training and evaluation. We train a face embedding model using CosFace [34] loss, ResNet-101 [10] backbone and DeepGlint-Face dataset (including MSIM-DeepGlint and Asian-DeepGlint) [5]. In Sec. 2.2.1, we use the HAC clustering algorithm [4] to cluster embeddings extracted from faces in the WIDERFace [42] dataset to obtain the UI cluster and its average embedding for ERS⁴. We select the threshold $\gamma = 0.60$ for ERS via cross-validation on the TinyFace [37] benchmark.

3.1. Evaluation data and metric

Single-image and set based face recognition experiments are run on the IARPA Janus Benchmark-C (IJB-C) [23]

⁴WIDER Face is a dataset for face detection, collected by daily event queries on the internet, and therefore highly unlikely to overlap with face recognition benchmarks, which are usually collected by celebrity queries.

| Method | Backbone | Train Data | IJB-C Verification (1-TAR)@FAR | | | |
|--------------------|------------------------------------------------|-------------|--------------------------------|---------------|---------------|---------------|
| | | | 1e-5 | 1e-4 | 1e-3 | 1e-2 |
| Multicolumn [40] | ResNet50 | VGGFace2 | 0.2290 | 0.1380 | 0.0730 | 0.0320 |
| DCN [39] | ResNet50 | VGGFace2 | - | 0.1150 | 0.0530 | 0.0170 |
| PFE [30] | 64-Layer CNN | MS-Celeb-1M | 0.1036 | 0.0675 | 0.0451 | 0.0283 |
| DUL [1] | ResNet64 | MS-Celeb-1M | 0.0977 | 0.0539 | 0.0530 | - |
| NAN [41] | ResNet64 trained with Cosface Loss | DeepGlint | 0.1023 | 0.0582 | 0.0347 | 0.0206 |
| Baseline (AvePool) | ResNet64 trained with Cosface Loss | DeepGlint | 0.1262 | 0.0639 | 0.0332 | 0.0165 |
| ERS | | | 0.0929 | 0.0547 | 0.0312 | 0.0157 |
| Baseline (AvePool) | ResNet101 trained with Sub-Center Arcface Loss | DeepGlint | 0.0592 | 0.0406 | 0.0271 | 0.0157 |
| ERS | | | 0.0528 | 0.0363 | 0.0245 | 0.0159 |

Table 1. Benchmark results on IJB-C template-based verification. On top, we compare using ERS for aggregation with the baseline of averaging embedding (AvePool) and other face aggregation methods. The results are reported at different FAR levels. We report error rates to better illustrate the difference between methods. ERS is also effective on the latest embedding model (Sub-Center ArcFace).

⁵. IJB-C is a benchmark suite that contains in-the-wild celebrity media, including photos and videos, and multiple predefined benchmarking protocols. We use four protocols from IJB-C: 1) **IJB-C Covariate Face Verification Test** for single-image based face verification; 2) **IJB-C Template-based Face Verification** for set-based face verification; 3) **IJB-C Template-based Face Search** for set-based face search; 4) **IJB-C Test10: Wild Probe with Full Motion Video Face Search** for set-based face search in videos. It is worth noting that the IJB-C Test10 contains video frames with strong motion blur, forming an FR testbed with the presence of unrecognizable video faces.

Evaluation Metric The performances of our methods are measured on two standard testing protocols for face recognition: 1:1 verification and 1:N search. For 1:1 face verification, we measure $1 - \text{true acceptance rate}$ ($1 - \text{TAR}$), also known as false reject rate (FRR), at a set of false acceptance rates (FARs). For 1:N face search, we measure $1 - \text{true positive identification rates}$ ($1 - \text{TPIR}$) at different false positive identification rates (FPIR), as well as the top- K rank accuracy.

3.2. ERS in Single Image-Based Face Verification

The IJB-C Covariate Test protocol (Table 2) benchmarks single-image based face verification. We evaluate our approach using Eq. 3 on this benchmark. We compare with FaceQnet [12] and SER-FIQ [32] ⁶ as the alternatives for face recognizability measure. With the same embedding model, using ERS as the recognizability measure (Eq. 3) leads to 58% error reduction comparing to that of not considering recognizability. The alternative recognizability

⁵This paper contains or makes use of the following data made available by the Intelligence Advanced Research Projects Activity (IARPA): Benchmark C (IJB-C) data detailed at Face Challenges homepage. For more information see <https://nigos.nist.gov/datasets/ijbc/request>.

⁶We used the **implementation** from SER-FIQ [32] to get prediction scores, during which we also adapt their preferred face detector and face embedding model from **Insightface**.

| Mehod | Verification (1-TAR)@FAR | | | |
|-----------------------------------|--------------------------|---------------|---------------|---------------|
| | 1e-6 | 1e-5 | 1e-4 | 1e-3 |
| Baseline | 0.6976 | 0.4540 | 0.1747 | 0.0714 |
| FaceQnet [12] ($\gamma = 1.00$) | 0.6976 | 0.4540 | 0.1747 | 0.0714 |
| SER-FIQ [32] ($\gamma = 0.83$) | 0.4027 | 0.2023 | 0.1164 | 0.0717 |
| ERS ($\gamma = 0.60$) | 0.3819 | 0.1885 | 0.1113 | 0.0673 |

Table 2. Comparison of recognizability conditioned face verification on IJBC Covariate Verification benchmark. We compare with FaceQnet [12] and SER-FIQ [32] as the alternatives for face recognizability measure. (As best thresholds are not suggested from the other works, we densely tested multiple thresholds and select their best results for comparison.)

measure FaceQnet cannot improve the baseline at all thresholds, and SER-FIQ is able to help reduce errors, but with less effect.

3.3. ERS in Set-Based Face Recognition

We evaluate set-based face recognition using ERS as described in Sec. 2.2.3. Results on the IJB-C Template-Based Face Verification and Search are illustrated in Table 1 (top). We adapt media-pooling [3] in set-based benchmarks. We compare ERS based method to the baseline of simple averaging without considering recognizability (AvePool). We also compare our approach with other methods developed for set-based face recognition. It can be seen that our approach significantly reduces recognition errors of the baseline. Our results are comparable or better than other complex methods developed for set-based recognition.

We also evaluate ERS on the IJB-C Test10 benchmark to test our algorithms on videos in-the-wild and implement an average pooling baseline and learning-based method NAN [41] for comparison. The results are summarized in Table 3. It can be seen that although obtained from images, ERS is also able to improve recognition accuracy in challenging video data.

Improving state-of-the-art face embedding models. In Fig. 1 we illustrate the UI cluster using the Cosface [34] for

| Method | Identification (1-TPIR)@FPIR | | | | Rank-N Error | |
|--------------------|------------------------------|---------------|---------------|---------------|---------------|---------------|
| | 1e-4 | 1e-3 | 1e-2 | 1e-1 | 1 | 5 |
| Baseline (AvePool) | 0.8607 | 0.6840 | 0.4129 | 0.2029 | 0.1564 | 0.1137 |
| NAN | 0.8566 | 0.6697 | 0.3726 | 0.1956 | 0.1518 | 0.1100 |
| ERS | 0.8299 | 0.6096 | 0.3054 | 0.1807 | 0.1457 | 0.1055 |

Table 3. IJB-C Test 10: Wild Probe with Full Motion Video Face Search results, tested using backbone ResNet101 trained on DeepGlintFace with CosFace [34] loss. In comparison with baseline average pooling and NAN [41] trained on top of the same backbone model, our ERS-based aggregation achieves the best performance.

embedding. The UI clustering phenomenon is not limited to that embedding model. We empirically find that multiple other face embedding models have similar behaviors, despite their different loss functions, size of training datasets, and backbone architectures. We conjecture that the existence of UI clusters may be attributed to the nature of face recognition as a fine-grained categorization task. Since ERS is easy to obtain for any face embedding model without extra training or annotation, we test applying ERS to multiple state-of-the-art face embedding models trained under different settings, including (1) loss function designs: Sub-center ArcFace [7], Softmax+Center Loss [38] and ℓ_2 -Softmax Loss [26]; (2) training dataset: IMDB [33] and DeepGlintFace; (3) backbone architectures: ResNet-101, ResNet-50 and ResNet-34 [10].

Results on the IJB-C face verification benchmark are illustrated in Fig. 6. We observe consistent error reduction on all tested models, including 10% error reduction at FAR=1e-5 on strong baseline from Sub-center ArcFace [7]. Full results can be found in Table 1 (bottom). This suggests that the ERS can be an easy plug-in to existing face recognition systems to reduce recognition errors.

3.4. Ablation study

Generation of the UI centroid. The UI representation is originally generated on the full WIDERFace [42] dataset. We compare the ERSs computed by UI representation generated on Fddb [13] and 3 random non-overlapping subsets of the WIDERFace [42]. Results in table 4 suggest that regardless of the source datasets, the UI centroid generated are very close in terms of Euclidean distance or cosine similarity. This also proves that ERS is not sensitive to the sources of the unrecognizable images.

| | WF split 1 | WF split 2 | WF split 3 | Fddb |
|------------|------------|------------|------------|---------|
| WF split 1 | - | 0.00098 | 0.00075 | 0.04163 |
| WF split 2 | - | - | 0.00079 | 0.04290 |
| WF split 3 | - | - | - | 0.03906 |

Table 4. Euclidean distance between UI centroid obtained from different data, including 3 distinct splits of WIDER Face [42] (WF) dataset and Fddb [13] dataset.

Choice of the weighting function w . Using ERS in set-based face recognition requires a choice of the weighting

function w . We compare different choices of w , including identity, exponential, and square on the IJB-C Template-Based Face Verification benchmark. We also compare with two special choices that average the images with top-1% and top-10% ERSs within a set. From table 5 we can see square function achieves the best results. We use it in other experiments without special notes.

| Weight function | e_i | $\text{softmax}(e_i)$ | e_i^2 | e_i | e_i |
|------------------|--------|-----------------------|---------------|--------|---------|
| Set Selection | N/A | N/A | N/A | top 1 | top 10% |
| (1-TAR)@FAR 1e-5 | 0.0684 | 0.1393 | 0.0627 | 0.2196 | 0.2025 |

Table 5. Comparison between different ERS-based aggregation methods on IJBC Templated-based Face Verification benchmark, basenet ResNet101 trained with Cosface [34].

3.5. Exploration on increasing ERS

Higher ERSs usually associate with faces with better recognizability. It is interesting to explore whether we can increase the ERS of a given image. We present the results of a naive method for this: enhance the face feature by removing its projection on the direction of the UI representation to yield high ERS ($e = 1$) features. Formally, we take the raw feature embedding \mathbf{f} , unit vector \mathbf{f}_{UI} and calculate the feature

$$\mathbf{v}^{id} = \mathbf{f} - \langle \mathbf{f}, \mathbf{f}_{UI} \rangle \mathbf{f}_{UI}. \quad (7)$$

After ℓ_2 normalization we get the ERS-enhanced features \mathbf{f}^{id} . From table 6 we can see average pooling with ERS-enhanced features surpasses the baseline by a large margin and achieves comparable results to ERS weighted aggregation. This suggests increasing embedding ERS can make a meaningful difference in benchmark results, achieving higher ERS through more advanced techniques may lead to a further increase in recognition accuracy.

| | (1-TAR)@FAR | | | |
|------------------------|---------------|---------------|---------------|---------------|
| | 1e-5 | 1e-4 | 1e-3 | 1e-2 |
| Baseline (AvePool) | 0.1140 | 0.0468 | 0.0264 | 0.0141 |
| ERS (WeightedPool) | 0.0627 | 0.0393 | 0.0243 | 0.0140 |
| ERS-Enhanced (AvePool) | 0.0644 | 0.0410 | 0.0255 | 0.0144 |

Table 6. Comparison among average pooling, ERS weighted pooling and average pooling with ERS enhanced features on IJBC Templated-based Face Verification benchmark, basenet is ResNet101 trained with Cosface [34].

3.6. Exploration on other vision tasks

As an extended study, we explore clustering on person re-identification (re-id) and image retrieval to see whether the low recognizability clustering phenomenon exists and our method can be applied accordingly. We perform re-id embedding clustering on Market1501 [44] dataset which contains low recognizability examples labeled “junk” and “distractors” in its gallery set. And likewise for partially



Figure 7. Similar to our findings in face clustering, miscellaneous low recognizability examples can gather in one cluster in person re-id (top, using Market1501 [44] dataset) and fashion retrieval datasets (bottom, using Deepfashion [19] dataset).



Figure 8. Images from Market1501 grouped by high, medium, low ERS scores. Positive correlation between recognizability and ERS can be observed.

perturbed Deepfashion [19] In-Shop dataset (most image retrieval datasets do not contain natural quality corruption, so we manually perturb the recognizability, similar to Fig. 4). In Fig. 7, we observe low recognizability miscellaneous samples can gather in one cluster similar to those of faces. After devising the associated ERS measures, it can be observed from Fig. 8 and Fig. 9 that consistent with our findings on the face, the ERS also correlates with the input image recognizability.

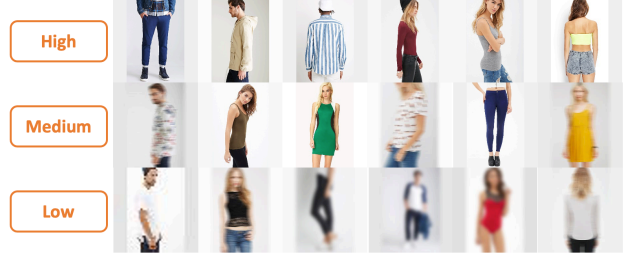


Figure 9. Images from Deepfashion with synthetic corruption grouped by high, medium, low ERS scores. Positive correlation between recognizability and ERS can be observed.

4. Discussion

Face recognition is subject to a vast array of issues that can affect the quality of its result. While we acknowledge the presence and importance of statistical and algorithmic biases, in this paper we focus on additional issues that exist even before any dataset is collected, and affects systems that are not trained on data. Simply put, some images contain sufficient information to ascertain that there *is* a face, but insufficient to determine *whose* face it is. This gap is captured by the concept of “recognizability”, which is affected by physical properties of the subject (sub-surface scattering and pigmentation, hairdo, accessories, makeup), but also extrinsic properties of the scene such as the nature and quality of the illuminant, physical properties of the sensor, calibration and pre-processing algorithms performed by the camera software, imaging conditions such as large aperture/high capture time resulting in motion blur, finite depth of field and resulting optical blur, just to mention a few.

We also acknowledge that the principled solution to both cascading failures of the detection, as well as recognizability of the detected face, is to properly marginalize the corresponding latent variables. Since that is highly impractical, we settle to the intermediate inference of recognizability, through the proposal of an admittedly ad-hoc measure, suggested by the manifest clustering of unrecognizable identities. Because of the issues mentioned above, and also verified empirically, the UI is a highly heterogeneous cluster. It includes images subject to wildly varying nuisance variability, unlike other domains such as large-scale image classification, where optical-blurred images form a cluster separate from motion-blurred images, also separate from low-resolution images. We also observe that images of different populations present in the UI.

With all due caveats in mind, we observe that explicitly accounting for recognizability through the admittedly unprincipled method we have proposed, we still achieve significant error reduction in face recognition on standard public benchmarks, and effectively allow a system to operate in an open-set setting without the complications of full-fledged open universe training.

References

- [1] Jie Chang, Zhonghao Lan, Changmao Cheng, and Yichen Wei. Data uncertainty learning in face recognition. In *Proceedings of the IEEE/CVF Conference on Computer Vision and Pattern Recognition*, pages 5710–5719, 2020. 3, 4, 5, 6
- [2] Tianqi Chen, Mu Li, Yutian Li, Min Lin, Naiyan Wang, Minjie Wang, Tianjun Xiao, Bing Xu, Chiyuan Zhang, and Zheng Zhang. Mxnet: A flexible and efficient machine learning library for heterogeneous distributed systems. *arXiv preprint arXiv:1512.01274*, 2015. 5
- [3] Nate Crosswhite, Jeffrey Byrne, Chris Stauffer, Omkar Parkhi, Qiong Cao, and Andrew Zisserman. Template adaptation for face verification and identification. *Image and Vision Computing*, 79:35–48, 2018. 6
- [4] William HE Day and Herbert Edelsbrunner. Efficient algorithms for agglomerative hierarchical clustering methods. *Journal of classification*, 1(1):7–24, 1984. 3, 5
- [5] Deepglint. <http://trillionpairs.deepglint.com/overview>. 5
- [6] Jia Deng, Wei Dong, Richard Socher, Li-Jia Li, Kai Li, and Li Fei-Fei. Imagenet: A large-scale hierarchical image database. In *2009 IEEE conference on computer vision and pattern recognition*, pages 248–255. Ieee, 2009. 4
- [7] Jiankang Deng, Jia Guo, Tongliang Liu, Mingming Gong, and Stefanos Zafeiriou. Sub-center arcface: Boosting face recognition by large-scale noisy web faces. In *Proceedings of the IEEE Conference on European Conference on Computer Vision*, 2020. 3, 7
- [8] Jiankang Deng, Jia Guo, and Stefanos Zafeiriou. Arcface: Additive angular margin loss for deep face recognition. *2019 IEEE/CVF Conference on Computer Vision and Pattern Recognition (CVPR)*, pages 4685–4694, 2018. 3
- [9] Sixue Gong, Yichun Shi, and Anil K Jain. Video face recognition: Component-wise feature aggregation network (c-fan). *arXiv preprint arXiv:1902.07327*, 2019. 3
- [10] Kaiming He, Xiangyu Zhang, Shaoqing Ren, and Jian Sun. Deep residual learning for image recognition. In *Proceedings of the IEEE conference on computer vision and pattern recognition*, pages 770–778, 2016. 5, 7
- [11] Javier Hernandez-Ortega, Javier Galbally, Julian Fierrez, and Laurent Beslay. Biometric quality: Review and application to face recognition with faceqnet. *arXiv preprint arXiv:2006.03298*, 2020. 3
- [12] Javier Hernandez-Ortega, Javier Galbally, Julian Fierrez, Rudolf Haraksim, and Laurent Beslay. Faceqnet: Quality assessment for face recognition based on deep learning. In *2019 International Conference on Biometrics (ICB)*, pages 1–8. IEEE, 2019. 3, 5, 6
- [13] Vedit Jain and Erik Learned-Miller. Fddb: A benchmark for face detection in unconstrained settings. Technical report, UMass Amherst technical report, 2010. 7
- [14] Muwei Jian and Kin-Man Lam. Simultaneous hallucination and recognition of low-resolution faces based on singular value decomposition. *IEEE Transactions on Circuits and Systems for Video Technology*, 25:1761–1772, 2015. 3
- [15] Weiyang Liu, Yandong Wen, Zhiding Yu, Ming Li, Bhiksha Raj, and Le Song. Spheroface: Deep hypersphere embedding for face recognition. *2017 IEEE Conference on Computer Vision and Pattern Recognition (CVPR)*, pages 6738–6746, 2017. 3
- [16] Xiaofeng Liu, Zhenhua Guo, Site Li, Lingsheng Kong, Ping Jia, Jane You, and BVK Kumar. Permutation-invariant feature restructuring for correlation-aware image set-based recognition. In *Proceedings of the IEEE/CVF International Conference on Computer Vision*, pages 4986–4996, 2019. 3
- [17] Xiaofeng Liu, BVK Kumar, Chao Yang, Qingming Tang, and Jane You. Dependency-aware attention control for unconstrained face recognition with image sets. In *Proceedings of the European Conference on Computer Vision (ECCV)*, pages 548–565, 2018. 3
- [18] Yu Liu, Junjie Yan, and Wanli Ouyang. Quality aware network for set to set recognition. In *Proceedings of the IEEE Conference on Computer Vision and Pattern Recognition*, pages 5790–5799, 2017. 3
- [19] Ziwei Liu, Ping Luo, Shi Qiu, Xiaogang Wang, and Xiaoou Tang. Deepfashion: Powering robust clothes recognition and retrieval with rich annotations. In *Proceedings of IEEE Conference on Computer Vision and Pattern Recognition (CVPR)*, June 2016. 4, 8
- [20] Boyu Lu, Jun-Cheng Chen, and Rama Chellappa. Unsupervised domain-specific deblurring via disentangled representations. *2019 IEEE/CVF Conference on Computer Vision and Pattern Recognition (CVPR)*, pages 10217–10226, 2019. 3
- [21] Ze Lu, Xudong Jiang, and Alex Chichung Kot. Deep coupled resnet for low-resolution face recognition. *IEEE Signal Processing Letters*, 25:526–530, 2018. 3
- [22] Laurens van der Maaten and Geoffrey Hinton. Visualizing data using t-sne. *Journal of machine learning research*, 9(Nov):2579–2605, 2008. 1
- [23] Brianna Maze, Jocelyn Adams, James A Duncan, Nathan Kalka, Tim Miller, Charles Otto, Anil K Jain, W Tyler Niggel, Janet Anderson, Jordan Cheney, et al. Iarpa janus benchmark-c: Face dataset and protocol. In *2018 International Conference on Biometrics (ICB)*, pages 158–165. IEEE, 2018. 5
- [24] Alice J O’Toole, Carlos D Castillo, Connor J Parde, Matthew Q Hill, and Rama Chellappa. Face space representations in deep convolutional neural networks. *Trends in cognitive sciences*, 22(9):794–809, 2018. 2
- [25] Omkar M. Parkhi, Andrea Vedaldi, and Andrew Zisserman. Deep face recognition. In *BMVC*, 2015. 3
- [26] Rajeev Ranjan, Carlos D Castillo, and Rama Chellappa. L2-constrained softmax loss for discriminative face verification. *arXiv preprint arXiv:1703.09507*, 2017. 7
- [27] Yongming Rao, Ji Lin, Jiwen Lu, and Jie Zhou. Learning discriminative aggregation network for video-based face recognition. In *Proceedings of the IEEE international conference on computer vision*, pages 3781–3790, 2017. 3
- [28] Karl Ricanek and Tamirat Tesafaye. Morph: A longitudinal image database of normal adult age-progression. In *7th International Conference on Automatic Face and Gesture Recognition (FG06)*, pages 341–345. IEEE, 2006. 11

- [29] Florian Schroff, Dmitry Kalenichenko, and James Philbin. Facenet: A unified embedding for face recognition and clustering. *2015 IEEE Conference on Computer Vision and Pattern Recognition (CVPR)*, pages 815–823, 2015. 3
- [30] Yichun Shi, Anil K Jain, and Nathan D Kalka. Probabilistic face embeddings. *arXiv preprint arXiv:1904.09658*, 2019. 3, 4, 5, 6
- [31] Yichun Shi, Xiang Yu, Kihyuk Sohn, Manmohan Chandraker, and Anil K Jain. Towards universal representation learning for deep face recognition. In *Proceedings of the IEEE/CVF Conference on Computer Vision and Pattern Recognition*, pages 6817–6826, 2020. 3
- [32] Philipp Terhorst, Jan Niklas Kolf, Naser Damer, Florian Kirchbuchner, and Arjan Kuijper. Ser-fiq: Unsupervised estimation of face image quality based on stochastic embedding robustness. In *Proceedings of the IEEE/CVF Conference on Computer Vision and Pattern Recognition*, pages 5651–5660, 2020. 3, 5, 6
- [33] Fei Wang, Liren Chen, Cheng Li, Shiyao Huang, Yanjie Chen, Chen Qian, and Chen Change Loy. The devil of face recognition is in the noise. In *Proceedings of the European Conference on Computer Vision (ECCV)*, pages 765–780, 2018. 7
- [34] Hao Wang, Yitong Wang, Zheng Zhou, Xing Ji, Dihong Gong, Jingchao Zhou, Zhifeng Li, and Wei Liu. Cosface: Large margin cosine loss for deep face recognition. In *Proceedings of the IEEE Conference on Computer Vision and Pattern Recognition*, pages 5265–5274, 2018. 1, 3, 5, 6, 7
- [35] Mei Wang and Weihong Deng. Deep face recognition: A survey. *ArXiv*, abs/1804.06655, 2018. 3
- [36] Zhangyang Wang, Shiyu Chang, Yingzhen Yang, Ding Liu, and Thomas S. Huang. Studying very low resolution recognition using deep networks. *2016 IEEE Conference on Computer Vision and Pattern Recognition (CVPR)*, pages 4792–4800, 2016. 3
- [37] Zhifei Wang, Zhenjiang Miao, QM Jonathan Wu, Yanli Wan, and Zhen Tang. Low-resolution face recognition: a review. *The Visual Computer*, 30(4):359–386, 2014. 5
- [38] Yandong Wen, Kaipeng Zhang, Zhifeng Li, and Yu Qiao. A discriminative feature learning approach for deep face recognition. In *European conference on computer vision*, pages 499–515. Springer, 2016. 3, 7
- [39] Weidi Xie, Li Shen, and Andrew Zisserman. Comparator networks. In *Proceedings of the European Conference on Computer Vision (ECCV)*, pages 782–797, 2018. 3, 5, 6
- [40] Weidi Xie and Andrew Zisserman. Multicolumn networks for face recognition. *arXiv preprint arXiv:1807.09192*, 2018. 3, 5, 6
- [41] Jiaolong Yang, Peiran Ren, Dongqing Zhang, Dong Chen, Fang Wen, Hongdong Li, and Gang Hua. Neural aggregation network for video face recognition. In *Proceedings of the IEEE conference on computer vision and pattern recognition*, pages 4362–4371, 2017. 3, 5, 6, 7
- [42] Shuo Yang, Ping Luo, Chen Change Loy, and Xiaoou Tang. Wider face: A face detection benchmark. In *IEEE Conference on Computer Vision and Pattern Recognition (CVPR)*, 2016. 3, 4, 5, 7
- [43] Jian Zhao, Yu Cheng, Yan Xu, Lin Xiong, Jianshu Li, Fang Zhao, Karlekar Jayashree, Sugiri Pranata, Shengmei Shen, Junliang Xing, et al. Towards pose invariant face recognition in the wild. In *Proceedings of the IEEE conference on computer vision and pattern recognition*, pages 2207–2216, 2018. 3
- [44] Liang Zheng, Liye Shen, Lu Tian, Shengjin Wang, Jingdong Wang, and Qi Tian. Scalable person re-identification: A benchmark. In *Proceedings of the IEEE international conference on computer vision*, pages 1116–1124, 2015. 4, 7, 8

Appendix: Bias analysis and discussion

In Sec. 1.3, we discussed the potential implication of biases, here we conduct some preliminary bias analysis of the proposed face recognizability prediction.

Test dataset and models We use Morph [28] dataset as our test data for the analysis, basic statistics of the dataset are shown in Table 7. Within each gender and ethnicity subgroup, we sample genuine and imposter 1v1 pairs to establish face verification benchmark protocol with gender and ethnicity breakdown.

We test on two face embedding models previously used in benchmark experiments, one being our reference *CosFace* embedding model (ResNet101 + CosFace Loss + DeepGlintFace), the other being the *SC-Arc* model (ResNet101 + Sub-center Arcface Loss + DeepGlintFace) which has the best performance on IJB-C.

| | | Gender | | Total |
|-----------|----------|--------|--------|--------|
| | | Female | Male | |
| Ethnicity | African | 24898 | 155783 | 180681 |
| | Asian | 536 | 1150 | 1686 |
| | European | 109132 | 99093 | 208225 |
| | Hispanic | 1880 | 8908 | 10788 |
| | Indian | 66 | 322 | 388 |
| | Other | 82 | 93 | 175 |
| | Unknown | 10 | 102 | 112 |
| | Total | 136604 | 265451 | 402055 |

Table 7. Morph [28] dataset image statistics breakdown by Gender / Ancestry .

Recognizability prediction distribution

We plot the recognizability prediction in *raw ERS*: $e_{raw} = 1 - \langle \mathbf{f}_{UI}, \mathbf{f}_i \rangle$, that is, we remove the cap-at-1 operation of ERS in Eq.1 for the convenience of observing the raw distribution. We show e_{raw} density distribution on Morph dataset for CosFace model in Fig. 10, and for SC-Arc model in Fig. 11. 95% confidence interval (CI) is computed through bootstrapping of 1000 iterations.

Verification benchmark

We also test and show face verification benchmark results with gender and ethnicity breakdown on Morph dataset for CosFace model in Table. 8, and for SC-Arc model in Table. 9.

Our interpretations of the preliminary results are as follows:

(1) Density distribution of each gender and ethnicity group are similar, especially when confidence intervals are considered. Gender and ethnicity do not appear to be significant causative or differentiating factors to the raw ERS distribution. The difference in the distributions may be attributed to the particularity of the model evaluated and random fluctuations in the data, rather than systematic biases of the method design. This is evidenced by that across two models, we do not observe one group to consistently have a

higher or lower prediction in general.

(2) Albeit there could be biases in these models according to verification results, the differences among groups only matter little in the application of the ERS we proposed. The proposed ERS yields high prediction (>0.8) for most images, regardless of the labeled gender and ethnicity. The chosen threshold of 0.6 barely incurs false positive prediction of recognizability across all these groups.

(3) The raw ERS distributions do not reveal a strong

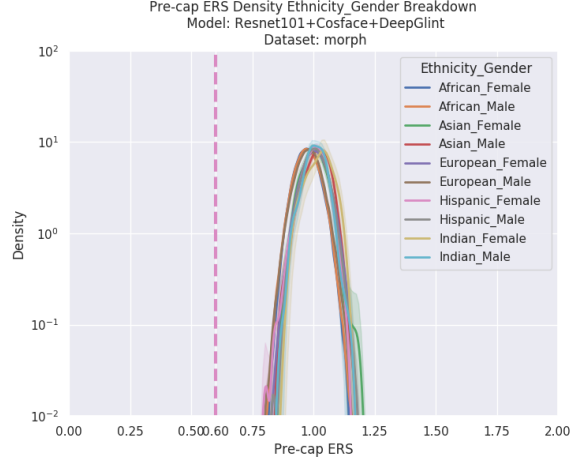


Figure 10. Density distribution of *raw ERS* ($e_{raw} = 1 - \langle \mathbf{f}_{UI}, \mathbf{f}_i \rangle$) on Morph dataset, with gender and ethnicity breakdown. Vertical dash indicates selected threshold at 0.6. 95% confidence interval depicted around each curve in lighter color. Y-axis shown in log scale. Model: reference CosFace (ResNet101 + CosFace Loss + DeepGlintFace). Please view in color.

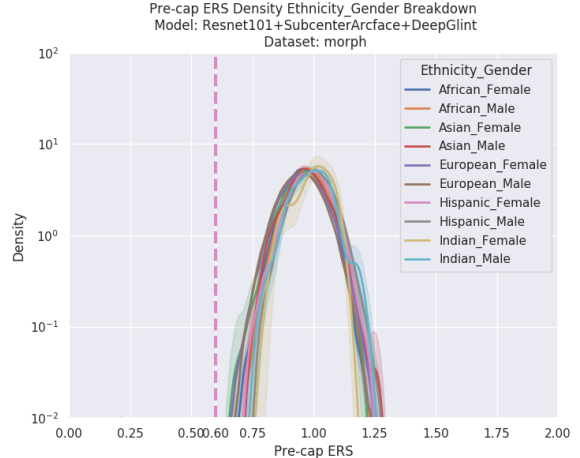


Figure 11. Density distribution of *raw ERS* ($e_{raw} = 1 - \langle \mathbf{f}_{UI}, \mathbf{f}_i \rangle$) on Morph dataset, with gender and ethnicity breakdown. Vertical dash indicates selected threshold at 0.6. 95% confidence interval depicted around each curve in lighter color. Y-axis shown in log scale. Model: SC-Arc (ResNet101 + Sub-center Arcface Loss + DeepGlintFace). Please view in color.

| FAR | $(1 - \text{TAR}) @ \text{FAR} = 1e-2$ | $(1 - \text{TAR}) @ \text{FAR} = 1e-3$ |
|-----------------|----------------------------------------|----------------------------------------|
| African_Female | 0.00021 | 0.00091 |
| African_Male | 0.00015 | 0.00022 |
| Asian_Female | 0.00218 | 0.00437 |
| Asian_Male | 0.00000 | 0.00000 |
| European_Female | 0.00046 | 0.00058 |
| European_Male | 0.00028 | 0.00030 |
| Hispanic_Female | 0.00061 | 0.00061 |
| Hispanic_Male | 0.00020 | 0.00035 |

Table 8. Reference CosFace model (ResNet101 + CosFace Loss + DeepGlintFace) breakdown 1v1 face verification benchmark on Morph dataset. (“indian” and “other” not tested due to insufficient number of images.)

| FAR | $(1 - \text{TAR}) @ \text{FAR} = 1e-2$ | $(1 - \text{TAR}) @ \text{FAR} = 1e-3$ |
|-----------------|----------------------------------------|----------------------------------------|
| African_Female | 0.00019 | 0.00023 |
| African_Male | 0.00018 | 0.00019 |
| Asian_Female | 0.00218 | 0.00218 |
| Asian_Male | 0.00000 | 0.00000 |
| European_Female | 0.00048 | 0.00052 |
| European_Male | 0.00030 | 0.00030 |
| Hispanic_Female | 0.00061 | 0.00061 |
| Hispanic_Male | 0.00025 | 0.00025 |

Table 9. Reference SC-Arc model (ResNet101 + Sub-center Arcface Loss + DeepGlintFace) breakdown 1v1 face verification benchmark on Morph dataset. (“indian” and “other” not tested due to insufficient number of images.)

correlation with the model’s face verification performance in each subgroup. This is evidenced by, for example, “Asian_Female” group has the highest error rate in both models, but its raw ERS distribution does not stand out among the curves.

It is worth noting that although the breakdown face verification results imply some biases of the face embedding models used, our investigation is far from thorough, given fairness is not the focus of this work. For more comprehensive analyses, we refer readers to the dedicated literature on face representation learning fairness analysis.